Published in "Advanced Optical Materials doi: 10.1002/adom.201300415, 2013"
which should be cited to refer to this work.

Silicon Hyperuniform Disordered Photonic Materials with a Pronounced Gap in the Shortwave Infrared

*Nicolas Muller, Jakub Haberko, Catherine Marichy, and Frank Scheffold**

Photonic crystals are metamaterials designed to display a periodic modulation of the refractive index.[1,2] For light wavelengths that match the Bragg condition, such materials display a photonic gap. For sufficient refractive index contrast, a complete band gap emerges, the density of states in the gap is zero, transmission vanishes and incident light is specularly reflected. The concept was initially proposed by Yablonovitch and John 25 years ago. Research in the field initially developed rapidly but has matured over the last decade. Although materials with complete band gaps have been reported from the infrared to the visible, there still exist many challenges in fabrication and for possible applications.[3,4] For example only recently three-dimensional guiding of photons in photonic crystals has been demonstrated.[5,6]

Interestingly disordered photonic structures are also candidates for complete band gap materials. Numerical data show that peculiar hyperuniform disordered materials can display complete bandgaps in two dimensions[7] that allows the design of cavities and optical waveguides.[8] Recent experimental data for two-dimensional hyperuniform structures in the microwave regime provide support for these claims.[9,10] Independent numerical calculations suggest that these concepts can also be applied to three-dimensional hyperuniform structures where a band gap is predicted to open for refractive indices $n \geq 3$ in air.[11] Here we present such hyperuniform structures made from silicon with a broad and pronounced gap in the shortwave infrared for the first time.

One of the intrinsic shortcomings of photonic crystals is the highly selective reflection from Bragg planes due to crystalline symmetries. For many practical applications this feature is detrimental. For example dye-free reflective color displays, colored packing materials or cosmetics are preferentially non-iridescent and thus non-crystalline. Moreover the design of optical integrated devices is based on the realization of waveguides, switches and optical cavities that suffer from the anisotropic optical response of crystalline solids.[8] While initially largely ignored, the design of amorphous photonic materials has gained increasing attention over the last decade.[12–16] Disordered dielectric structures with short-range order display wide-angle reflection and broad spectral features. Early experiments demonstrated that the transmission and reflection properties are governed by an interplay between Mie scattering and local order via the modulation of the single scattering cross section.[13,14] To some extent both properties can be tuned independently which in turn allows to tailor solid and liquid materials with a specific optical response, finding use in random lasers[15] or for materials where angle-independent structural colors are desired.[16] While engineering disordered photonic materials is just at its beginning, many examples can already be found in nature such as in non-iridescent colors of bird feathers,[17] or brilliant whiteness in beetle scales.[18]

For a photonic crystal of thickness L the sum of transmittance T and specular reflectance R is $T + R = 1$, for energies below the onset of diffraction.[19] Thus in a crystal specular reflection is high in the vicinity of the gap wavelength λ_G and the transmittance displays an exponential decay $T = e^{-L/L_B}$, where L_B is the Bragg length. This is the reason underlying the iridescence of crystalline materials such as opal gems. As a consequence specular reflection is often used as a robust measure to characterize photonic properties for example in sensing applications.[20] Disordered materials intrinsically show a very different behavior. In disordered dielectrics transmittance always decays exponentially and the characteristic attenuation length is the scattering mean free path $l_s(\lambda)$.[13,14,16] At the same time reflection is broad rather than being peaked in one direction.

We now turn out attention to hyperuniform disordered photonic materials. To provide perspective, we first introduce the concept of hyperuniformity. A point pattern in three dimensions is hyperuniform when number fluctuations $\langle N_R^2 \rangle - \langle N_R \rangle^2$ in a spherical window R grow more slowly than the window volume ~ R^3.[21] This means density fluctuations vanish on large length scales or small q-vectors in reciprocal space and thus the structure factor $S(|\boldsymbol{q}| \to 0) \to 0$. Crystals and quasicrystals display sharp peaks in q-space and thus trivially are all hyperuniform but not isotropic.[9] Disordered point patterns however can be isotropic *and* hyperuniform. A well-studied example is given by the center positions of jammed hard spheres having a diameter a,[22,23] also known as random close packing (RCP).[24] Such point patterns display a pronounced structure peak at $q = 2\pi/a$ and vanishing scattering in the forward direction $q \to 0$. It is worthwhile to point out that this is a photonic feature of many dense repulsive packings with important consequences for biology, for the transparency of the mammalian eye lens,[25] and for the optical appearance of complex fluids, such as emulsions and nanoemulsion.[26] In order to achieve the strongest possible photonic response (for a given refractive index contrast)

N. Muller, Dr. J. Haberko,
Dr. C. Marichy, Prof. F. Scheffold
Department of Physics and Fribourg
Center for Nanomaterials
University of Fribourg
Chémin du Musée 3, 1700, Fribourg, Switzerland
E-mail: Frank.Scheffold@unifr.ch
Dr. J. Haberko
Faculty of Physics and Applied Computer Science
AGH University of Science and Technology
al. Mickiewicza 30, 30–059, Krakow, Poland

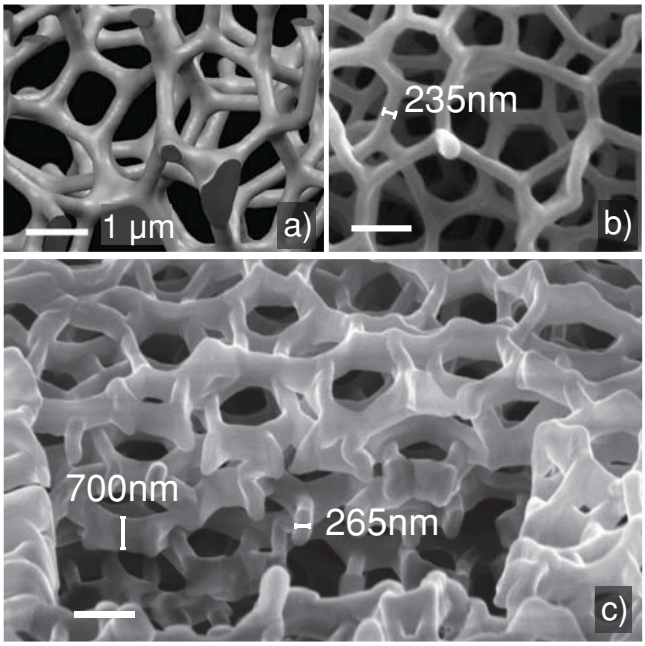

Figure 1. Electron micrographs of mesoscale silicon hyperuniform disordered structures. (a) Computer generated image of the structure (b) Top view of a h = 6 µm structure silicon infiltrated for 9 min. (c) Close-up oblique view of a focused ion beam cut of the same structure reveals the interior structure of solid rods and the absence of voids. The size of the silicon-coated rods with an elliptic cross-section of approximately 250 × 700 nm^2 (in-plane) indicates a volume filling fraction of $\phi \approx 0.15$. All scale bars are 1 µm.

the optimal combination of global structural properties and local scattering properties has to be found. To this end Florescu, Torquato and Steinhardt propose network structures that possess long range hyperuniform structural correlations combined with a uniform local topology and short-range order.[7] Numerical calculations suggest that for a sufficient refractive index contrast the resulting materials display a complete photonic band gap. Moreover the relation between the structural and the photonic properties has been mapped out for two and three dimensions.[7,11]

In the present work we use the center positions from a jammed assembly of spheres with diameter $a = 2$ µm taken from[23] as a seed pattern and translate it numerically into a hyperuniform (HU) network structure as described in.[27] Note that the choice of a sets the characteristic length scale of the structure and thus the position of the gap λ_G. Briefly, the design protocol consists in constructing tetrahedrons by drawing lines between adjacent points of the seed pattern and subsequently connecting the centroids of the tetrahedrons resulting in a 3D disordered network of rods with the desired structural properties. Finally we prepare a three-dimensional representation based on realistic assumptions about the shape of the laser writing pen (**Figure 1**a).[11] From this digital representation we also derive a relation between the volume filling fraction ϕ and the mean diameter of the rods $\langle D \rangle : \phi \approx 3.5(\langle D \rangle / a)^2, \phi \leq 0.4$. The mean diameter $\langle D \rangle$ is defined as the root of the product of the long and the short axis of the ellipsoidal laser writing pen.[27]

Next we discuss the fabrication of high refractive index mesoscale network materials based on computer-generated line structures, Figure 1a. We use direct laser writing (DLW) into a liquid photoresist to create polymer templates of the network structures as reported previously[22,27] (**Figure 2**a). The polymer templates are very open since the initial polymer-filling fraction is about 15% only for a typical rod size of $\langle D_P \rangle \sim$ 400–500 nm.[22,27] In order to mechanically stabilize the network at higher temperatures we first coat the polymer structure with a thin TiO_2

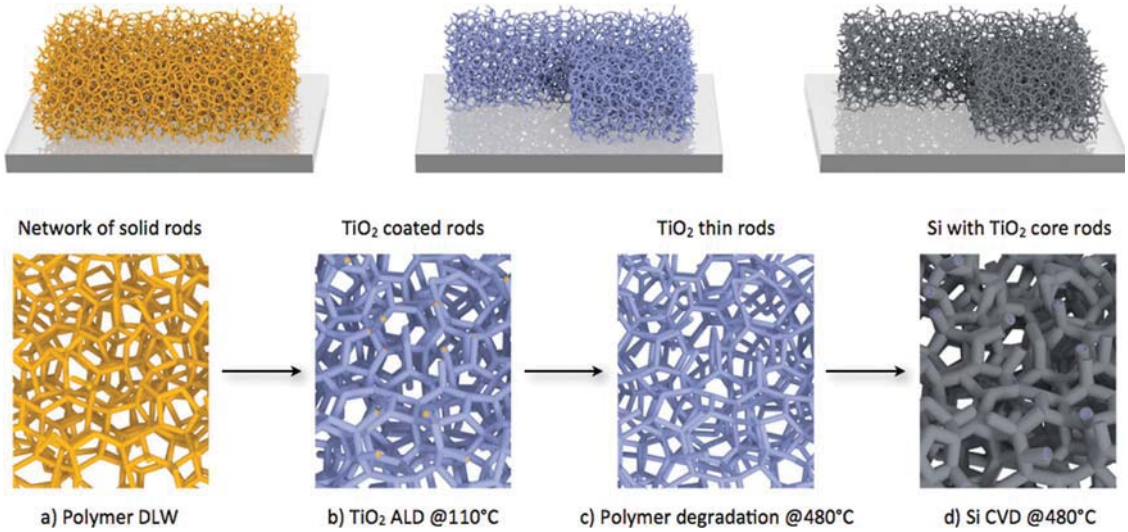

Figure 2. Procedure to fabricate silicon replica of mesoscale polymeric templates obtained by direct laser writing (DLW) lithography. (a) Polymer template of a network structure obtained by direct laser writing (DLW) (b) Polymer network coated with a thin, ca. 8 nm, layer of TiO_2 to mechanically stabilize the network using atomic layer deposition (ALD) at a moderate temperature of 110 °C. (c) Thermal degradation of the polymer at 480 °C results in a ultra low density network of TiO_2 rods with filling fraction $\phi_0 \sim 4\%$. d) By chemical vapor deposition of silicon at 480 °C we fabricate hyperuniform silicon networks at volume filling fractions $\phi = 0.15 \rightarrow 0.4$. The silicon rods retain a small TiO_2 core.

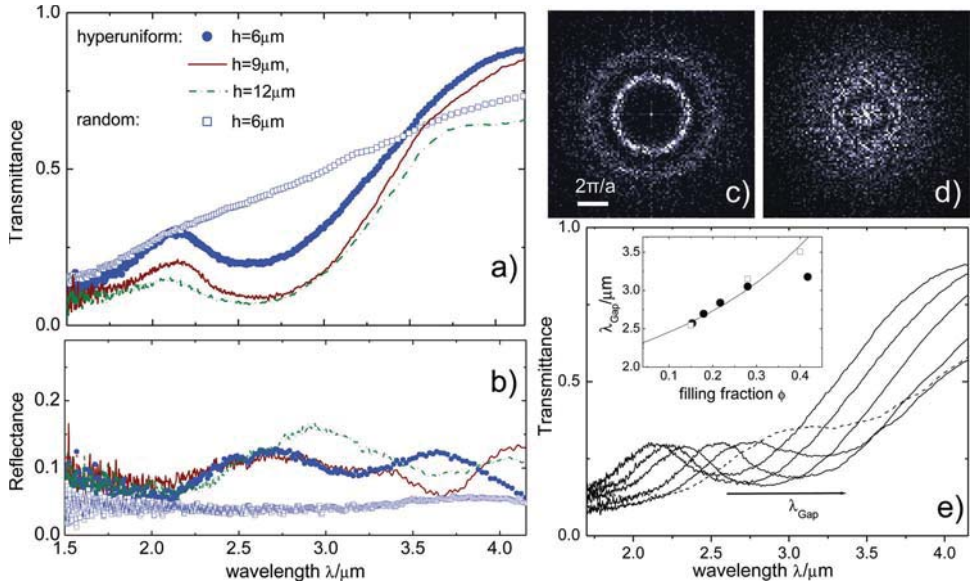

Figure 3. Infrared photonic response of silicon hyperuniform network structures. (a,b) Transmittance and reflectance spectra for hyperuniform structures of different heights h = 6–12 μm and for a random structure h = 6 μm infiltrated with silicon for t = 9 min ($\phi \approx 0.15$). (c,d) Cross section at q_z = 0 of the 3D scattering function $I(\boldsymbol{q}) \sim S(\boldsymbol{q})$ for the hyperuniform network and for the random network.[11,22] (e) Red-shift of the gap wavelength λ_{Gap} for h = 6 μm and its progression with subsequent silicon deposition steps via CVD (solid lines: 9, 10.5, 12.5, 15.5, 21 min infiltration from left to right, or $\phi \approx 0.15 \rightarrow 0.42$, dashed line: 27 min). Inset shows the evolution of λ_{Gap} (full symbols) compared to the numerical predictions for silicon rods (open symbols) reported in the literature[11] and for a_{eff} = 1.6 μm. The solid line shows the model prediction $\lambda_{Gap} = n_{eff}(\phi) \times \lambda_0$ assuming a constant silicon surface deposition rate of β = 11 nm/minute as explained in the text, with λ_0 = 2.25 μm.

layer ($n \sim 2.5$)[3,13] by depositing a roughly 8 nm film of TiO_2 at a moderate temperature of 110 °C using atomic-layer-deposition (ALD), (Figure 2b). Next, the polymer is thermally degraded by keeping the sample at a temperature of 480 °C for about 20–30 min (Figure 2c, see also Figure SI-1). Electron microscopy confirms that the network structure remains intact and we do not observe hollow rods. This suggests that we obtain a network of essentially pure TiO_2. If we assume that the TiO_2-density of the coating layer and of the rods is roughly the same we can estimate the TiO_2 rod-diameter: $\pi(\langle D_T \rangle / 4)^2 \approx \pi \langle D_P \rangle \cdot 8\,nm$ and obtain $\langle D_T \rangle \sim 220$ nm.[28] For an aspect ratio of about 2.8 the mean rod thickness $\langle D_T \rangle \sim 220$ nm translates into an approximate short axis length of 130 nm, in good agreement with electron microscopy (see also Figure SI-2, SI-3). Moreover the corresponding value for the TiO_2 filling fraction $\phi_0 \sim 4\%$ agrees well with elemental analysis of the final material by Energy Dispersive Spectroscopy (Table SI-1). Subsequent to the thermal treatment we use chemical vapor deposition (CVD)[5,29] at 480 °C to infiltrate the ultra-low density TiO_2 network structure with silicon ($n \sim 3.6$)[30] (Figure 2d). Figure 1 shows the high-quality silicon positive replica of the original hyperuniform polymer structure. From the electron micrographs we also extract the approximate shape parameters of the rods. Oriented in-plane[22] the rods are elliptical with a long axis of length approximately 700 nm and a short axis of 250 nm, thus $\langle D \rangle \sim \sqrt{250 \cdot 700}$ nm = 418 nm, which provides an estimate for the filling fraction $\phi \sim 15\%$. From this we estimate the residual TiO_2 content to about 25% with a mean refractive index of the rods $n \sim 3.3$.

To determine the transmission and reflection spectra we use a Fourier transform infrared microscope-spectrometer. The microscope employs a pair of Cassegrain lenses with acceptance angles spread + /–10° relative to the incident direction and 10°–30° relative to the surface normal and thus in our measurements we probe a band of reciprocal wave vectors. However, due to the structural isotropy, the angular spread will have little influence on the results for the transmittance data. We observe a pronounced photonic gap in the optical transmittance at $\lambda_{Gap} \sim 2.6$ μm that extends from $\lambda \sim 2.2$–3 μm, **Figure 3**a. In parallel we observe enhanced reflection over a broad range of wavelengths. Increasing the height of the samples has little influence on the reflection properties but further reduces transmittance. For comparison we also fabricate networks starting from a random seed pattern that does not show short-range order and is not hyperuniform. To illustrate the different structural properties we plot in Figure 3c,d a cross section of the 3D scattering function for both cases. Our experiments clearly show that for the random structures the spectra are featureless and no gap is observed, Figure 3a. Moreover the reflectance is found to be substantially lower, Figure 3b.

Next we investigate how the optical response depends on the silicon-filling fraction ϕ or silicon infiltration time t. To this end we deposit step-wise additional amounts of silicon on top of existing structures. As a result the gap position continuously shifts to higher wavelengths, Figure 3e, and eventually the gap is reduced to a shoulder after t = 27 min. Up to t = 21 min, or filling fractions $\phi \leq 0.42$, this shift can be modeled assuming a constant growth rate of β = 11 nm/min and a corresponding increase of $\phi(t)$. As shown in Figure 3e we can estimate the effective refractive index $n_{eff}(\phi)$ of the materials using the Bruggeman mixing formula,[31] which in turn provides a quantitative prediction for the gap wavelength $\lambda_G = n_{eff}(\phi)\lambda_0$

and its dependence on infiltration time. The only adjustable parameter is $\lambda_0 \sim 2.25$ μm, the gap position in the limit $n_{\text{eff}} \rightarrow 1$ (air). Numerical calculations for the same kind of 3D hyperuniform network structures[11] show that a complete photonic band gap opens up for refractive indices $n \geq 3$ and for filling ratios $\phi = 0.15$–0.4. In agreement with the numerical results we find the gap most pronounced for $\phi = 0.2$–0.3, while its strength decreases for higher filling ratios. Moreover we can directly compare the position of the gap $\lambda_G(\phi)$ observed experimentally with the numerical results for $\phi = 0.15$, 0.28, 0.4 reported in the literature[11] for the case of pure silicon rods with n = 3.6. As shown in Figure 3e we find excellent agreement for slightly reduced structural length scale $a_{eff} \sim 1.6$ μm. At least some of the difference, as compared to the seed pattern with $a = 2$ μm, can be attributed to the well-known shrinkage of structures during development,[32] thermal polymer degradation and high temperature Si-infiltration.

The structural characterization, the spectral response and the comparison to numerical calculations show that we have produced high quality disordered photonic materials made of silicon at a solid filling fraction $\phi = 0.15$–0.42. Our results thus suggest that these structures do possess a complete photonic band gap. Nonetheless the presence of scattering and the wide-angle reflection in disordered structures renders an experimental proof for a complete gap difficult. In practice one would need to measure the density of states directly using fluorescent local probes.[33] Alternatively one could analyze the integrated transmission, the transverse spreading of an incident light beam,[34] speckle fluctuations or the distribution of scattering paths.[35] Such experiments are beyond the scope of the present work but shall be attempted in the future. Finally we would like to emphasize that photonic properties of disordered dielectric materials have also been studied in the context of strong multiple scattering and Anderson localization of light.[35,36] Recent theoretical work indicates the absence of light localization in a completely random ensemble of scatterers[37] and thus supports the idea that spatial correlations are a necessary condition for achieving Anderson localization of light in three dimensions. This implies that Anderson localization would be confined to a well defined spectral range, dictated by structural correlations with the spatial frequency a.[2] Moreover the conditions required to achieve a complete gap, such as the refractive index contrast ($n \geq 3$) and filling fraction, appear to be very similar to those contemplated for Anderson localization of light.[13,35,38] It is thus likely that the emergence of band gaps and localized states in disorderd dielectrics are strongly connected.[2] Unfortunately, to date, a general theoretical description of the optical transport in disordered photonic materials is not yet available.

In conclusion we have, for the first time, fabricated hyperuniform disordered photonic materials made from silicon that do possess all the properties required for a complete band gap to open up as predicted by theory.[11] Our experiments confirm the presence of a pronounced gap in the shortwave infrared and we can quantitatively describe the red-shift of the gap wavelength upon increasing the silicon filling fraction. The experimentally observed gap wavelengths are also found in good agreement with the predictions by numerical calculations[11] Although our results suggest the presence of a complete gap additional experiments are still required for an unequivocal proof due to the difficulties arising from the competition between classical scattering processes and the opening of a complete gap in disordered photonic materials.

Experimental Section

Direct-Laser Writing (DLW): We used the center positions from a jammed assembly of spheres taken from[23] and translated it numerically into a hyperuniform (HU) network structure as described previously.[27] Random networks were derived from the center position of a random assembly of spheres at a much lower volume-filling fraction of 5%. Next mesoscale polymer templates were fabricated using a commercial direct laser-writing (DLW) platform (Photonic Professional from Nanoscribe GmbH, Germany) in the Dip-In configuration as described previously.[22,27] Structures were written on IR transparent CaF_2 substrates (Crystan, UK) by *dipping* the objective directly inside a liquid negative-tone photoresist (IP-DIP, Nanoscribe, Germany) and by fine-tuning the laser power. Two successive development baths in PGMEA (Propylene glycol monomethyl ether acetate) for twice 10 min and a consecutive bath in isopropanol for 8 min were chosen. The structures were dried gently by redirecting a stream of N_2 through a bubbler containing isopropanol.

Titanium Dioxide ALD: A thin TiO_2 layer was deposited on the HU structures by ALD from titanium isopropoxide (Sigma-Aldrich, 97% purity) and DI water, as metal and oxygen source, respectively. Depositions took place at 110 °C in a commercial ALD reactor (Savannah 100, Cambridge Nanotech, Inc.) operating in exposure mode. Metal precursor and water were introduced subsequently by pneumatic ALD valves from their reservoirs, which were kept at 80 °C and room temperature, respectively. Under a carrier gas flow of 5 sccm, the ALD valves were opened for 0.02 and 0.05 s for the oxygen source and titanium precursor, respectively. The residence time, after each pulse, without N_2 flow and the following purge time under 20 sccm of N_2 were set to 20 s and 90 s, respectively. Considering a nominal growth per cycle of 0.8 Å, 100 cycles were applied.

Silicon CVD: The TiO_2 coated HU structures were subsequently infiltrated with Si by thermal CVD. The deposition took place at 480 °C in a custom built reactor working with a base pressure of 9 Torr. The structures were slowly raised in temperature, with plateaus at 150, 250, 350, and 480 °C, with a dwelling time between 15–30 min, in order to stabilize the structure and to thermally degrade the polymer. Subsequently Disilane (Si_2H_6) was added as a precursor. The precursor flow was controlled with a flow meter and set at 2 sccm. For the deposition, the flow was maintained for 9 minutes at 14 torr. The deposition rate using a slightly different design for the reaction chamber, and for a precursor flow of 1 sccm, was reported to be approximately 6 nm per minute.[29] Due to the higher precursor flow we expect a growth rate of the order $\beta = 10$–15 nm/min. Subsequent annealing of the silicon structures at 600 °C did not lead to measureable differences in the transmittance spectra.[39]

For a constant growth rate β we can estimate the volume deposition $d\phi/dt = \beta A/V$ using the surface to volume ratio of an assembly of cylindrical rods $A/V = 2\phi/R(\phi)$ with an approximate initial (TiO_2) filling fraction ϕ_0: $= \phi_{t=0} = 0.04$ and a corresponding mean rod diameter $\langle D_T \rangle = 2\langle R \rangle_{t=0} \sim 220$ nm. Solving this equation leads to the following expression $\phi(t) = [(\alpha t)^2 + 4\alpha t\sqrt{\phi_0} + 4\phi_0]$ with $\alpha = 2\beta\sqrt{14}/a$, (with $a = 2$ μm). Here we have used $\phi \approx 3.5(\langle 2R \rangle / a)^2$. Since ϕ (9 min) ≈ 0.15, see Figure 1, we obtain a value $\beta \approx 11$ nm/min for the deposition rate.

Increasing the infiltration time leads to a red shift of the gap wavelength $\lambda_G(\phi) = n_{\text{eff}}(\phi)\ \lambda_0$ as shown in Figure 3e. To model this dependence we calculate the refractive index of silicon coated rods n_{rod} as a function of the Si content as well as the effective refractive index of the bulk material using the Bruggeman mixing formula.[31] As shown in Figure 3d we find good agreement up to an infiltration time $t = 21$ min or $\phi \approx 0.42$ with $\lambda_0 = 2.25$ μm as the only adjustable parameter. Note that over the range $t = 9 \rightarrow 21$ min the effective index of the rods increases

from $n_{rod} = 3.3 \rightarrow 3.5$ and the bulk effective refractive index $n_{eff} = 1.15 \rightarrow 1.65$.

Structural Characterization: The structures were investigated with scanning electron microscopy (SEM) and cross-sections were realized by focused ion beam milling using a Dualbeam NOVA600 Nanolab (FEI). The etching was realized with a Ga ion beam with an acceleration of 30 kV at a current of 3 nA for a couple of minutes followed by a "cleaning" at 30 kV and 1 nA beam.

Optical Characterization: Measurements of the optical response of the structures were taken with a Fourier transform IR spectrometer (Bruker Vertex 70) coupled to a microscope (Bruker Hyperion 2000, liquid N_2-cooled InSb detector). The objective was a 36× Cassegrain, numerical aperture 0.52. The transmittance of light incident at an angle between 10 and 30° to the normal was analyzed. Spectra were normalized on the same substrate as the residing structures and on a gold mirror for transmittance and reflection measurements, respectively.

Supporting Information

Supporting Information is available

Acknowledgements

The present project has been financially supported by the National Research fund, Luxembourg (project No. 3093332), the Swiss National Science Foundation (projects 132736 and 149867) and the Adolphe Merkle Foundation. JH acknowledges financial support from a Sciex Swiss Research Fellowship No. 10.030. We would like to thank Frédéric Cardinaux, Stefan Guldin and Martin Hermatschweiler for fruitful discussions and Christoph Neururer for help with the scanning electron microscopy.

[1] a) J. D. Joannopoulos, *Photonic Crystals: Molding the Flow of Light*, Princeton University Press, Princeton **2008**; b) E. Yablonovitch, *Phys. Rev. Lett.* **1987**, *58*, 2059.
[2] S. John, *Phys. Rev. Lett.* **1987**, *58*, 2486.
[3] C. M. Soukoulis, M. Wegener, *Nat. Photonics* **2011**, *5*, 523.
[4] C. Lopez, J. F. Galisteo-Lopez, M. Ibisate, R. Sapienza, L. S. Froufe-Perez, A. Blanco, *Adv. Mater.* **2011**, *23*, 30.
[5] K. Ishizaki, M. Koumura, K. Suzuki, K. Gondaira, S. Noda, *Nat. Photonics* **2013**, *7*, 133.
[6] S. A. Rinne, F. Garcia-Santamaria, P. V. Braun, *Nat. Photonics* **2008**, *2*, 52.
[7] M. Florescu, S. Torquato, P. J. Steinhardt, *Proc. Natl. Acad. Sci. USA* **2009**, *106*, 20658.
[8] M. Florescu, P. J. Steinhardt, S. Torquato, *Phys. Rev. B* **2013**, *87*, 165116.
[9] W. N. Man, M. Florescu, K. Matsuyama, P. Yadak, G. Nahal, S. Hashemizad, E. Williamson, P. Steinhardt, S. Torquato, P. Chaikin, *Opt. Express* **2013**, *21*, 19972.
[10] W. N. Man, M. Florescu, E. P. Williamson, Y. Q. He, S. R. Hashemizad, B. Y. C. Leung, D. R. Liner, S. Torquato, P. M. Chaikin, P. J. Steinhardt, *Proc. Natl. Acad. Sci. USA* **2013**, *110*, 15886.
[11] S. F. Liew, J. K. Yang, H. Noh, C. F. Schreck, E. R. Dufresne, C. S. O'Hern, H. Cao, *Phys. Rev. A* **2011**, *84*, 063818.
[12] P. D. Garcia, R. Sapienza, C. Lopez, *Adv. Mater.* **2010**, *22*, 12.
[13] M. Reufer, L. F. Rojas-Ochoa, S. Eiden, J. J. Saenz, F. Scheffold, *Appl. Phys. Lett.* **2007**, 91, 171904.
[14] L. F. Rojas-Ochoa, J. M. Mendez-Alcaraz, J. J. Saenz, P. Schurtenberger, F. Scheffold, *Phys. Rev. Lett.* **2004**, *93*, 171904.
[15] K. Y. Jeong, Y. H. Lee, H. Cao, J. K. Yang, *Appl. Phys. Lett.* **2012**, *101*, 091101.
[16] S. Magkiriadou, J. G. Park, Y. S. Kim, V. N. Manoharan, *Opt. Mater. Express* **2012**, *2*, 1343.
[17] V. Saranathan, J. D. Forster, H. Noh, S. F. Liew, S. G. J. Mochrie, H. Cao, E. R. Dufresne, R. O. Prum, *J. R. Soc. Interface* **2012**, *9*, 2563.
[18] P. Vukusic, B. Hallam, J. Noyes, *Science* **2007**, *315*, 348.
[19] a) F. Garcia-Santamaria, J. F. Galisteo-Lopez, P. V. Braun, C. Lopez, *Phys. Rev. B* **2005**, *71*, 195112; b) P. D. Garcia, R. Sapienza, L. S. Froufe-Perez, C. Lopez, *Phys. Rev. B* **2009**, *79*, 241109.
[20] N. Griffete, H. Frederich, A. Maitre, S. Ravaine, M. M. Chehimi, C. Mangeney, *Langmuir* **2012**, *28*, 1005.
[21] S. Torquato, F. H. Stillinger, *Phys. Rev. E* **2003**, *68*, 041113.
[22] J. Haberko, N. Muller, F. Scheffold, *Phys. Rev. A* **2013**, *88*, 043822.
[23] C. Song, P. Wang, H. A. Makse, *Nature* **2008**, *453*, 629.
[24] S. Torquato, T. M. Truskett, P. G. Debenedetti, *Phys. Rev. Lett.* **2000**, *84*, 2064.
[25] A. Stradner, G. Foffi, N. Dorsaz, G. Thurston, P. Schurtenberger, *Phys. Rev. Lett.* **2007**, *99*, 198103.
[26] S. M. Graves, T. G. Mason, *J. Phys. Chem. C* **2008**, *112*, 12669.
[27] J. Haberko, F. Scheffold, *Opt. Express* **2013**, *21*, 1057.
[28] It is possible that the network of TiO_2 rods after thermal degradation of the polymer is somewhat porous and rough which would result in slightly thicker TiO_2 rods. Most of this roughness or porosity however will be filled by silicon in the final infiltration step. Since the total TiO_2 content is known (see also Table SI-1) the mean index of the rods and thus photonic response of the material as a whole are largely unaffected by the exact size and porosity of the intermediate TiO_2 rod thickness.
[29] M. Hermatschweiler, A. Ledermann, G. A. Ozin, M. Wegener, G. von Freymann, *Adv. Funct. Mater.* **2007**, *17*, 2273.
[30] M. Janai, D. D. Allred, D. C. Booth, B. O. Seraphin, *Sol. Energ. Mater.* **1979**, *1*, 11.
[31] A. Sihvola, *Institution of Electrical Engineers. Electromagnetic Mixing Formulas and Applications*, Institution of Electrical Engineers, London **1999**.
[32] G. von Freymann, A. Ledermann, M. Thiel, I. Staude, S. Essig, K. Busch, M. Wegener, *Adv. Funct. Mater.* **2010**, *20*, 1038.
[33] P. Lodahl, A. F. van Driel, I. S. Nikolaev, A. Irman, K. Overgaag, D. L. Vanmaekelbergh, W. L. Vos, *Nature* **2004**, *430*, 654.
[34] H. Hu, A. Strybulevych, J. H. Page, S. E. Skipetrov, B. A. Van Tiggelen, *Nat. Phys.* **2008**, *4*, 945.
[35] D. S. Wiersma, *Nat. Photonics* **2013**, *7*, 188.
[36] F. Scheffold, D. Wiersma, *Nat. Photonics* **2013**, *7*, 934.
[37] S. E. Skipetrov, I. M. Sokolov, **2013**, arXiv:1303.4655 [physics.optics].
[38] F. J. P. Schuurmans, D. Vanmaekelbergh, J. van de Lagemaat, A. Lagendijk, *Science* **1999**, *284*, 141.
[39] I. Staude, M. Thiel, S. Essig, C. Wolff, K. Busch, G. von Freymann, M. Wegener, *Opt. Lett.* **2010**, *35*, 1094.